Improving Latent and Sensible Heat Flux Estimates for the Atlantic Ocean (1988–99) by a Synthesis Approach*

LISAN YU, ROBERT A. WELLER, AND BOMIN SUN+

Department of Physical Oceanography, Woods Hole Oceanographic Institution, Woods Hole, Massachusetts

(Manuscript received 15 November 2002, in final form 26 June 2003)

ABSTRACT

A new daily latent and sensible flux product developed at the Woods Hole Oceanographic Institution (WHOI) with 1° × 1° resolution for the Atlantic Ocean (65°S–65°N) for the period from 1988 to 1999 was presented. The flux product was developed by using a variational objective analysis approach to obtain best estimates of the flux-related basic surface meteorological variables (e.g., wind speed, air humidity, air temperature, and sea surface temperature) through synthesizing satellite data and outputs of numerical weather prediction (NWP) models at the National Centers for Environmental Prediction (NCEP) and the European Centre for Medium-Range Weather Forecasts (ECMWF). The state-of-the-art bulk flux algorithm 2.6a, developed from the field experiments of the Coupled Ocean–Atmosphere Response Experiment (COARE), was applied to compute the flux fields.

The study focused on analyzing the mean field properties of the WHOI daily latent and sensible heat fluxes and their comparisons with the ship-based climatology from the Southampton Oceanography Centre (SOC) and NWP outputs. It is found that the WHOI yearly mean fluxes are consistent with the SOC climatology in both structure and amplitude, but the WHOI yearly mean basic variables are not always consistent with SOC; the better agreement in the fluxes is due to the effects of error compensation during variable combinations. Both ECMWF and NCEP–Department of Energy (DOE) Atmospheric Model Intercomparison Project (AMIP) Reanalysis-2 (NCEP2) model data have larger turbulent heat loss (~20 W m^{-2}) than the WHOI product. Nevertheless, the WHOI fluxes agree well with the NCEP-2 Reanalysis fluxes in structure and the trend of year-to-year variations, but not with the ECMWF operational outputs; the latter have a few abrupt changes coinciding with the modifications in the model forecast–analysis system. The degree of impact of the model changes on the basic variables is not as dramatic, a factor that justifies the inclusion of the basic variables, not the fluxes, from the ECMWF operational model in the synthesis. The flux algorithms of the two NWP models give a larger latent and sensible heat loss. Recalculating the NWP fluxes using the COARE algorithm considerably reduces the strength but does not replicate the WHOI results. The present analysis could not quantify the degree of improvement in the mean aspect of the WHOI daily flux fields as accurate basinwide verification data are lacking.

This study is the first to demonstrate that the synthesis approach is a useful tool for combining the NWP and satellite data sources and improving the mean representativeness of daily basic variable fields and, hence, the daily flux fields. It is anticipated that such an approach may become increasingly relied upon in the preparation of future high-quality flux products.

1. Introduction

The need to develop high-quality, gridded, time-dependent, and basin-to-global-scale air–sea turbulent (latent and sensible) and radiative (shortwave and longwave) heat fluxes has been widely recognized (Taylor 2000). Such flux products are of great interest to the climate research community for modeling and understanding coupled variability of the atmosphere–ocean system and for providing initial and verification data for climate prediction models. At present, surface turbulent heat fluxes are usually estimated using a bulk algorithm that requires the knowledge of surface meteorological variables, such as near-surface wind speed, air and sea surface temperatures, near-surface specific humidity, and surface saturation humidity (e.g., Liu et al. 1979). Those flux-related variables are usually obtained from one of three sources: marine surface weather reports from Voluntary Observing Ships (VOSs), satellite remote sensing, and outputs of numerical weather prediction (NWP) models, such as those at the National Centers for Environmental Prediction (NCEP) and the European Centre for Medium-Range Weather Forecasts (ECMWF). Different sources provide different spatial

* Woods Hole Oceanographic Institution Contribution Number 10961.

+ Current affiliation: NOAA/National Climate Data Center, Asheville, North Carolina.

Corresponding author address: Dr. Lisan Yu, MS#21, Department of Physical Oceanography, Woods Hole Oceanographic Institution, Woods Hole, MA 02543.
E-mail: lyu@whoi.edu

coverages and resolutions and different sampling rates (or temporal resolutions), and those differences influence both temporal and spatial representativeness of resulting flux estimates. This can be seen from the following summary of the characteristics of the fluxes based on the three data sources.

- Marine ship reports compose the only quasi-global, multidecade, surface meteorology dataset and are the backbone for a number of climatological flux atlases (e.g., Bunker 1976; Esbensen and Kushnir 1981; Isemer and Hasse 1985, 1987; Hsiung 1986; Oberhuber 1988; da Silva et al. 1994; Josey et al. 1998). Although those climatologies are adequate to offer the first-order depiction of long-term mean heat exchange patterns at the air–sea interface, they are not sufficient to describe flux variability, even on monthly time scales. This is particularly true in regions such as the Indian Ocean and the Southern Ocean where ship routes are limited.
- Satellite-based global surface heat fluxes (e.g., Chou et al. 1995; Schulz et al. 1997; Curry et al. 1999; Kubota et al. 2003) are an attractive alternative to the VOS-based climatological fluxes because of the good temporal and spatial resolutions and continuous global coverage. Many air–sea variables, including surface wind speed and vector, SST, water vapor, rain rate, cloudiness, etc., can now be retrieved from satellites, which allow fluxes to be computed directly from bulk formulae. But the accuracy of satellite-based fluxes is often limited by the accuracy of retrieval algorithms. At present, retrieving air humidity at a level of several meters above the surface remains to be a major technical challenge (Schulz et al. 1993), and this has been a leading error source in satellite latent flux estimates (Simonot and Gautier 1989). Satellite-based fluxes also need to be verified with high accuracy in situ fluxes to adjust the biases induced by retrieval schemes.
- Surface flux products from the NWP models are gridded, global, and available continuously at 6-h intervals. However, the NWP fluxes at present contain a considerable degree of uncertainty arising from deficiencies in boundary layer parameterizations and related flux bulk algorithms (White 1995; Beljaars 1997; Siefridt et al. 1999). Validation studies (e.g., Weller and Anderson 1996; Moyer and Weller 1997; Weller et al. 1998; Josey 2001; Smith et al. 2001; Renfrew et al. 2002; Kubota et al. 2003; Sun et al. 2003) have found that the NWP turbulent heat fluxes are systematically overestimated. These biases pose a major obstacle to the application of NWP fluxes to climate studies.

It is clear that different flux products come with different advantages and limitations due to differences in data sources. Questions have been raised as to whether one can synthesize the advantage of each data source and produce a synthesized product with improved resolution and improved quality. Synthesis denotes the process of using an advanced objective analysis approach to combine measurements/estimates from various sources (Daley 1991). Such a process reduces the errors in data and produces an estimate that is optimal at the solution; that is, the estimate has the minimum error variance. Applications of the synthesis methodology have been made successfully to surface vector wind fields and SST fields (e.g., Legler et al. 1989; Atlas et al. 1993; Reynolds and Smith 1994). An attempt was also made to synthesize monthly latent and sensible heat fluxes over the Indian Ocean (e.g., Jones et al. 1995). In this paper, we report on our investigation of the use of a synthesis approach, namely, the variational objective analysis, to improve the estimates of turbulent latent and sensible heat fluxes on daily and 1° grid resolution for the Atlantic Ocean from 65°S to 65°N for the period of 1988–99. This paper represents the first part of an ongoing effort at the Woods Hole Oceanographic Institution (WHOI) to develop high-quality, gridded, time-dependent surface turbulent and radiative fluxes to support the Atlantic climate studies under the auspices of the National Oceanic and Atmospheric Administration (NOAA) Climate Variability and Predictability (CLIVAR) Atlantic program.

In developing a synthesized flux product, the first and foremost question is how to combine the advantages of existing data sources and improve the representation of both the mean and variability of the fluxes. Synthesizing directly the fluxes from satellite-derived and NWP-generated products is not a wise choice because they contain biases both from bulk algorithms and from flux-related surface meteorological variables, and the nonlinearity of boundary layer processes complicates the identification of error sources. Our starting point was that estimates of the fluxes could be improved if flux-related variables could be improved and a good-quality flux bulk algorithm is available. At present, the bulk algorithm 2.6a (Fairall et al. 1996; Bradley et al. 2000) developed from the field experiments of the Tropical Ocean Global Atmosphere Coupled Ocean–Atmosphere Response Experiment (TOGA COARE) (Webster and Lukas 1992) represents state-of-the-art flux parameterization. Therefore, we designed our strategy first to produce the best estimates of basic variables through synthesis and then to compute the flux fields using the COARE algorithm 2.6a. That is to say, the WHOI product resulted from using the best possible estimates of flux-related variables and the best possible flux algorithm.

The base (input) data used in the synthesis included satellite retrievals and outputs from the NCEP and ECMWF models. The satellite retrievals were the surface wind speed (Wentz 1997) and air humidity (Chou et al. 2003) from the Special Sensor Microwave Imager (SSM/I) and surface temperature from the Advanced Very High Resolution Radiometer (AVHRR) (Brown et al. 1993). The NCEP–Department of Energy (DOE).

Atmospheric Model Intercomparison Project (AMIP) Reanalysis 2 data (hereafter referred to as NCEP2) were synthesized instead of the NCEP–National Center for Atmospheric Research (NCAR) reanalysis 1 (hereafter referred to as NCEP1), because our previous study (Sun et al. 2003) found that NCEP2, an update of NCEP1, has an overall improvement in the estimates of not only T_a, q_a, and U, but also turbulent heat fluxes. The synthesis used the ECMWF operational forecast model outputs but not those from the 15-yr ECMWF Re-Analysis data (ERA-15) that are available from January 1979 to February 1994. The former model undergoes successive updates of parameterization schemes and data assimilation algorithms to seek the best possible analysis/forecast fields (Siefridt et al. 1999), unlike the reanalysis model that employs a frozen analysis–forecast system. However, we found that those updates have impacted more on the tendency of the flux variations and less on the tendency of the variations of the flux-related basic variables. The trend of year-to-year variations for basic variables agrees reasonably well with other products. This is the main reason that the variables from the ECMWF operational model can be used in the synthesis, in addition to the up-to-present coverage, which is long enough for the synthesis period from 1988 to 1999.

Ship meteorological reports, which constitute the database of the Comprehensive Ocean–Atmosphere Data Set (COADS) project, were not synthesized for the following reasons. First, the coverage of ship routes on a daily basis is extremely sparse compared with the global coverage of satellite retrievals or NWP model outputs. This significantly limits the influence of ship measurements on the estimation. Second, ship observations extend over multiple decades and are a good source for constructing climatological flux atlases. Last, the ship-based flux atlases could be a useful source of comparison data if ship data are excluded in the synthesis. However, the ship-based fluxes also have their own set of problems (Gleckler and Weare 1997). The flux climatology used in this study is the one from the Southampton Oceanography Centre (SOC: Josey et al. 1998). The monthly climatology, which was constructed from the COADS database and available for the period of 1980–97, has been shown to be the best flux climatology at present (Josey 2001; Sun et al. 2003; Toole et al. 2004, hereafter TZC). Yet, even the best climatology was constructed with many approximations and has considerable degrees of uncertainties. The biases are particularly large over a broad region centered on the Gulf Stream in the western North Atlantic (Josey et al. 1999).

In this paper, the methodology of the synthesis approach and its application to obtain best daily estimates of the basic variables required in the COARE algorithm are presented. The mean field properties of the WHOI fluxes and their comparisons with the SOC climatology and the NWP fluxes are discussed. The WHOI flux product has daily resolution. Its characteristics at daily time scales are included in a companion paper (Yu et al. 2003, manuscript submitted to *J. Climate*) that uses benchmark time series provided by in situ flux buoys as verification. The presentation of the study is organized as follows. Section 2 provides descriptions of the flux algorithm, data sources, and the methodology for formulating the variational objective analysis. Section 3 compares the mean properties of the WHOI fluxes with those from the SOC flux climatology analysis. Comparisons with the ECMWF and NCEP2 fluxes and variables are also presented. A summary and discussion are given in section 4.

2. Strategy, methodology, and data sources

a. Types of independent variables needed in the COARE algorithm 2.6

The bulk expressions of the latent and sensible heat fluxes, Q_{LH} and Q_{SH} are

$$Q_{\mathrm{LH}} = \rho L_e c_e U(q_s - q_a) \tag{1}$$

$$Q_{\mathrm{SH}} = \rho c_p c_h U(T_s - \theta), \tag{2}$$

where ρ is the density of air, L_e is the latent heat of evaporation, c_p is the specific heat capacity of air at constant pressure, U is the average value of the wind speed relative to the sea surface at the depth of z_r, c_e and c_h are the stability and height dependent turbulent exchange coefficients for latent and sensible heat, respectively, T_s is the sea surface skin temperature, θ is the near-surface air potential temperature, and q_s and q_a are the sea surface and near-surface atmospheric specific humidities, respectively. Note that q_s is computed from the saturation humidity, q_{sat}, for pure water at T_s,

$$q_s = 0.98 q_{\mathrm{sat}}(T_s), \tag{3}$$

where a multiplier factor of 0.98 is used to take into account the reduction in vapor pressure caused by a typical salinity of 34 psu. In addition, θ includes a correction for the adiabatic lapse rate, γ:

$$\theta = T_a + \gamma z_r, \tag{4}$$

where T_a is the air temperature at z_r.

Bulk algorithms differ in how roughness lengths and the transfer coefficients (c_e and c_h) are parameterized, and whether or not wave spectrum, convective gustiness, and salinity are considered (Zeng et al. 1998; Brunke et al. 2003). The version 2.6a of the COARE bulk algorithm included all of the issues except the effects of capillary waves in its development using the COARE measurements in the western tropical Pacific (Fairall et al. 1996). Since its publication, the algorithm has been used and tested under various conditions outside the tropical oceans, such as for colder waters, midlatitudes, and wind speed greater than 10 m s^{-1} (Bradley et al. 2000). The current COARE version is accurate within 5% for wind speeds of 0–10 m s^{-1} and 10% for wind speeds of 10–20 m s^{-1} (Fairall et al. 2003). Based upon direct turbulent flux measurements determined from co-

variance and inertial dissipation methods from 12 ship cruises over the tropical and midlatitude oceans (from about 5°S to 60°N), Brunke et al. (2003) showed that the overall performance of the COARE algorithm tops the other 11 algorithms considered.

In Eqs. (1)–(4), only U, T_s, T_a, and q_a are independent variables and they are to be estimated from the synthesis. All other variables, including the transfer coefficients, are determined based upon the information of the four variables and the specified parameterization. In the following, we denote U to be at 10 m, T_a and q_a at 2 m, and T_s at the sea surface so that the reference heights used in the synthesis are consistent with those used in the NWP models. For satellite retrievals that do not have the same reference heights as their NWP counterparts, the COARE 2.6a algorithm is applied to make the height adjustment.

b. Data sources

The synthesis uses surface wind speed U (Wentz 1997) and humidity q_a (Chou et al. 2003) at the 10-m reference height retrieved from the SSM/I, surface temperature from the AVHRR, and the outputs of U, T_s, T_a, and q_a from the ECMWF operational forecast and NCEP reanalysis–forecast models. A brief description of each of the data sources is given in the following.

1) THE NCEP2 REANALYSIS

NCEP2 is regarded as the update of NCEP1 and not a next-generation reanalysis. NCEP1 produces an ongoing dataset from 1948 to the present, while NCEP2 corrects known errors in NCEP1 and generates data from 1979 to the present. The two reanalysis systems use the same T62 L28 resolution, raw observed data, and turbulent flux algorithm, but differ largely in the parameterization of shortwave radiation and cloud and soil moisture (Kanamitsu 1989; Kanamitsu et al. 2000; Kalnay et al. 1996). Our previous study (Sun et al. 2003) compared the turbulent fluxes and flux-related variables from the NWP models with measurements from moored buoys in the Atlantic Ocean and found that NCEP2 has an overall improvement in the estimates of T_a, q_a, and U, and also turbulent heat fluxes. Therefore, the NCEP2 basic variable fields are chosen for our synthesis. These variable fields are on the Gaussian 192 × 94 grid (approximately 1.875° in longitude and latitude). Daily averages were processed.

2) THE ECMWF OPERATIONAL ANALYSIS

The daily ECMWF basic variables in use, which are available from 1985 to the present, are from the operational analysis system. The model grid is approximately 1.125° in both longitude and latitude. Unlike the ERA-15, which uses a frozen analysis forecast system, the ECMWF operational system seeks to obtain the best analysis/forecast fields through updating model parameterizations and data assimilation schemes so that it has the up-to-date parameterizations of air–sea fluxes (Beljaars 1997; Klinker 1997).

Over the synthesis period from 1988 to 1999, a few updates in the model parameterizations have major impacts on the tendency of the variations of surface turbulent heat fluxes. The moisture transfer coefficients were changed in 1990 for low wind speed and again in 1993 for high wind speed, which brought the latent heat flux up by about 20 W m^{-2} in the equatorial region (Siefridt et al. 1999). A modification in the data-handling techniques in December 1994–January 1995 gave a sudden reduction of 10 W m^{-2} at all latitudes. At the same time, temperature and humidity profiles obtained from the inversion of brightness temperature were implemented to replace the profiles retrieved from NOAA's Television Infrared Observation Satellite (TIROS) Operational Vertical Sounder (TOVS). The change also had a considerable impact on the surface fluxes in the Tropics (ECMWF 1994). The four-dimensional variational assimilation was operational in November 1997 (Rabier et al. 1998), and consequently, several improvements were made to the use of both conventional and satellite data. The assimilation of SSM/I total column water vapor was introduced and the assimilation of the scatterometer winds was revised, both of which directly affected the forecast of near-surface humidity and winds (Vesperini 1998) and indirectly affected the surface fluxes.

3) AVHRR SST

We use the NOAA–NASA Oceans Pathfinder SST product (Brown et al. 1993) rather than the optimal interpolated SST weekly analysis from Reynolds and Smith (1994), because the latter does not provide the needed daily variability. The Pathfinder product is derived from the five-channel AVHRR scanner that has been flown onboard the NOAA series of Polar Orbiting Operational Environmental Satellites (POESs) in sun-synchronous orbits since 1979. The five channels are located in the visible, near-infrared, and thermal infrared portions of the electromagnetic spectrum. Clouds have large effects on infrared measurements since they are opaque to infrared radiation and can effectively mask radiation from the ocean surface. Therefore, though the satellite orbits the earth 14 times each day from 833 km above its surface, and each pass of the satellite provides a 2399-km-wide swath, it usually needs 1 or 2 weeks, depending on the actual cloud coverage, to obtain a complete global coverage. The average SST retrieval has a root-mean-square (rms) difference of around 0.5°C (McClain et al. 1985). The daily field of the Pathfinder product is available with a spatial resolution of 9 km × 9 km but with significant data gaps due to cloud.

4) SSM/I WIND SPEED AND HUMIDITY

The SSM/I has been operating since July 1987 onboard a series of Defense Meteorological Satellite Program (DMSP) spacecraft in a circular sun-synchronous near-polar orbit at an altitude of approximately 860 km and orbit period of 102 min. The 1394-km swath of the SSM/I, only half of that of AVHRR, covers 82% of the earth's surface between 87°36′S and 87°36′N in 24 h and produces a complete coverage within 3 days (Halpern et al. 1994; Wentz 1997). SSM/I wind speed derived from the Wentz (1997) algorithm with a reference height at 10 m is used. The data are available at a resolution of 12 h and at a swath resolution of 25 km. Wind speeds are flagged if cloud/rain liquid water values exceed 18 mg cm^{-2} because the accuracy of the wind speed retrievals quickly degrades in the presence of rain. Wind speed values are also flagged if the measurements are within 50–100 km of the coast or within 200 km of the climatological mean monthly position of the ice edge because the validity of the algorithm is questionable over these areas. The SSM/I wind speeds have a rms difference of 1.6 m s^{-1} and zero bias as compared to buoy measurements (Wentz 1992).

The Wentz SSM/I product includes also total precipitable water over the open ocean. Schulz et al. (1993) obtained the precipitable water in the lower 500 m of the atmospheric planetary boundary layer using the brightness temperatures computed from the 19-GHz horizontal, and 19-, 22-, and 37-GHz vertical polarizations. By using estimates of the total and 0–500-m precipitable water, Chou et al. (1995, 1997) devised a retrieval technique to derive daily near-surface specific humidity based on the empirical orthogonal functions method. The derived surface humidity at 10 m has a rms difference of 1.83 g kg^{-1} estimated by SSM/I–radiosonde comparison. Daily fields with a spatial resolution of 1° latitude × 1° longitude are provided from version 2 of the Goddard Satellite-Based Surface Turbulent Fluxes (GSSTF) data (Chou et al. 1997).

c. The synthesis approach

The objective of the synthesis is to combine the fields of the basic flux variables given by the NCEP2 and ECMWF model analyses and satellite sensors and to obtain an optimal analysis field that is as close as possible to the true state in an rms sense (i.e., it is a minimum variance estimate). The methodology governing the synthesis is based on the Gauss–Markov theorem, a standard statistical estimation theory (Daley 1991) that has been widely used in meteorology (e.g., Gandin 1963) and oceanography (e.g., Bretherton et al. 1976). This theorem states that, when combining data in a linear fashion, the linear least squares estimator is the most efficient estimator and the solution has the minimum variance.

The application of the theory involves finding a minimum of an objective function that measures the lack of fit to a set of constraints. The objective function formulated for the problem in the present study takes the form

$$J = (X_e - FX_{\text{ana}})^{\text{T}} R_e (X_e - FX_{\text{ana}}) + (X_n - FX_{\text{ana}})^{\text{T}} R_n (X_n - FX_{\text{ana}}) + (X_s - FX_{\text{ana}})^{\text{T}} R_s (X_s - FX_{\text{ana}}) + \mu(\Delta X_{\text{ana}}/\Delta t)^2, \quad (5)$$

where the superscript "T" denotes transpose and F is a linear transformation function that maps the analysis field onto data positions; R_e, R_n, and R_s are the weights that are inversely proportional to the error covariances of the input data X_e, X_n, and X_s, respectively. The first three terms are data constraints that represent least squares fitting of the analysis vector field (X_{ana}) to the estimates of ECMWF (X_e), NCEP2 (X_n), and satellites (X_s), and the last term represents a priori information that ensures continuity between two consecutive daily fields (ΔX_{ana}). Here Δt is the time interval of 1 day, and μ is a scaling parameter, its value determined by the maximum change in X_{ana} given per Δt. For U, T_s, T_a, and q_a, μ was set to be the square of 12 m s^{-1} day^{-1}, 10°C day^{-1}, and 10°C day^{-1}, and 10 g kg^{-1} day^{-1}, respectively. The last term is a time evolution constraint, addressing the degree of acceptance for the differences between two consecutive daily fields. Its contribution to the minimization of J is at least one order smaller than the first three terms. Variations in μ had little effect on the results.

A conjugate–gradient method is used iteratively to find an optimal solution of the objective function J (Yu and O'Brien 1991, 1995). A similar approach was used by Legler et al. (1989) and Jones et al. (1995) to produce monthly surface flux analyses based on ship reports and by Atlas et al. (1993) to produce synthesized SSM/I wind vector fields with 6-hourly resolution. The analysis fields, X_{ana}, produced from (5) include U, T_s, T_a, and q_a on daily and 1° × 1° grid resolution. The SSM/I wind speed and humidity retrievals are available from July 1987 to present, the AVHRR SST are from November 1981 onward, the NCEP2 outputs are from January 1979 onward, and the ECMWF operational data outputs are from January 1985 onward. The synthesis focuses on the period between January 1988 and December 1999, the period during which all data sources can be included.

d. Sensitivity of the solution fields to the weight assignments

Error statistics for each input data field are needed to compute the error covariance matrix and determine the weight of each data constraint defined in (5). As the weights are inversely proportional to the error covariance matrices, the contribution of the input data to the analysis field is small if the errors are large and vice versa. So the weights determine the closeness of the fit between the analysis fields and input data fields. None

of the input datasets (i.e., ECMWF, NCEP, AVHRR, SSM/I) is equipped with information about error characteristics and distributions in space and time. Such information is difficult to obtain due to the lack of benchmark datasets over the basin scale. The problem was also experienced in the studies using a similar approach to obtain the blended wind stress fields (Legler et al. 1989; Atlas et al. 1993) and the monthly surface turbulent heat fluxes in the Indian Ocean (Jones et al. 1995), all of which were resolved by using constant weights invariant with time and space.

To determine reasonable weights for this study, we have constructed various weights and experimented with the response of the solution fields to the changes in amplitudes and spatial structures of the weights (Yu et al. 2002). The experiments tested constant weights, weights that are latitude dependent, and weights whose spatial structures are derived from using the SOC climatology of the global air–sea fluxes and surface meteorology. The monthly SOC climatology, which was constructed from the COADS database and available from 1980 to 1997, has been shown to be the best flux climatology at present (Josey 2001; Sun et al. 2003; TZC). Yet, even the best climatology was constructed with many approximations (Josey et al. 1998), which gives rise to considerable degrees of uncertainties (Gleckler and Weare 1997). Hence, the surface meteorology fields from the SOC can provide neither the ''true'' spatial structures in the NWP and satellite errors nor the true amplitude of those errors over basin scale. Nevertheless, we included them in the experiments to test the response of the solution fields to various, though not realistic, weight structures.

The constant weights and latitude-dependent weights were obtained from averaging the error fields. To minimize the uncertainties induced by sampling errors in the SOC analysis, the amplitudes of the weights were further fine-tuned using surface meteorological measurements from the buoys deployed by the WHOI Upper Ocean Processes group (e.g., Moyer and Weller 1997) and by the Pilot Research Moored Array in the Tropical Atlantic (PIRATA). These measurements provide high-quality data that can be used as benchmark time series for the purpose of verification. The amplitude tuning was done in the following way. We wrote the weighting matrices $\mathbf{R}$ in (5) as

$$\mathbf{R} = \alpha\overline{\mathbf{R}}, \tag{6}$$

where α are to-be-determined scalars and $\overline{\mathbf{R}}$ are the inversion of the time-invariant error variances estimated from using the SOC dataset. The α are estimated in a way that the left-hand side of Eq. (6) agrees with the mean averages of the inversion of the error variances at the buoy sites. By doing so, the amplitudes obtained for the weights of the 10-m wind speed for the NCEP2, ECMWF, and SSM/I fields are 2, 1, and 4, respectively. This implies that, on average, the ECMWF winds have errors about 1.4 times larger than NCEP2 and about 2 times larger than SSM/I. The amplitudes for all weights are listed in Table 1. In general, the satellite data were assigned with larger amplitudes because their standard deviations from the buoy data are smaller, and so the satellite data have larger contributions to the solution in (5).

TABLE 1. The amplitudes of the weights.

Weighting matrix	NCEP2	ECMWF	SSM/I	AVHRR
$\mathbf{R}(q_a)$	1	1	3	
$\mathbf{R}(T_a)$	2	1		
$\mathbf{R}(T_s)$	1	1		6
$\mathbf{R}(U)$	2	1	4	

The experiments showed that the changes in the solution fields induced by the three sets of weights are small (Yu et al. 2002). For U, q_a, and T_s, the differences between the experiments using different weights are less than 1% over the entire basin. For T_a, however, the influence of input data quality on the synthesis becomes evident. The differences between different experiments are small (less than 1%) for the region north of 40°S, but quite significant (reaching 10%) to the south of this latitude due to large uncertainty in the NWP models. The accuracy of the NWP models at high southern latitudes is limited, due to the lack of ship observations for constraining the models. Unlike other variables that have retrievals available from SSM/I and AVHRR, the input data sources for T_a include only the two NWP outputs.

On average, the analysis error in the flux estimation induced by uncertainties in the weights is less than 3 W m^{-2} for the latent flux and about 0.5 W m^{-2} for the sensible flux. Caution should be exercised in interpreting the sensible flux at high southern latitudes, where the analysis error can be on the order of 5 W m^{-2}. Because the weight-induced differences in the flux fields are negligible, the fluxes computed from the experiments using constant weights are presented in the following analysis.

The insensitivity of the solution fields to the weight assignments might be due to the fact that the number of input data points is about 2–3 times greater than the number of grid points in the analysis field. Each variable estimation included the synthesis of at least two NWP datasets plus available satellite retrievals from SSM/I and AVHRR. If errors in input data are reasonably confined (i.e., the error size of the variable is not of the same order as the total value of the variable itself), the optimization problem formulated in (5) should be well determined and the solution should be unique. That is to say, the quality of input data is a key in the synthesis. This is supported by the finding that the solution fields of T_a are sensitive to weights at higher southern latitudes, the region where errors in the NWP fields are large.

3. Comparisons of fluxes

In this section, we report on comparing the long-term mean field structures of the WHOI daily flux fields with the SOC flux climatology and with the NCEP2 and ECMWF model outputs. The efforts are to determine the compatibility between the WHOI flux product based on the synthesized fields and the one based on ship reports and to assess the differences between the synthesized product and the NWP outputs. The mean aspect of the flux fields is the focus of this study. The WHOI flux product has daily resolution. Evaluating temporal variability of the fluxes with in situ measurements from flux buoys and research vessels as verification data was presented in a recent study (YSW).

The construction of the WHOI product is different from that of the SOC product in three major ways. First, data sources are different. The input datasets for the SOC product came exclusively from the historic ship-based meteorological reports from COADS, while the WHOI analysis is based upon the synthesis of the flux-related variables from the NWP model outputs and satellite retrievals. Second, methodologies are different. The SOC analysis applied an averaging procedure and successive correction method to interpolate irregular temporal and spatial samplings onto regular grid points. The WHOI analysis is based upon an advanced variational objective analysis that combines data from different sources to produce the best possible estimate. Third, temporal resolutions are different. The SOC product emphasizes the climatological means, while the WHOI product is time dependent and has daily resolution. We are aware that computing the weights (the error variances) in the objective function (5) has referred to the SOC basic variables. However, the influence of the SOC data in the weights is rather limited because constant weights were used and the relative importance of each data source was determined by the error statistics at the buoy sites. Besides, the weights determine the closeness of the fit between the analysis field and the input data field; they represent a measure for the synthesis but not an input dataset. Furthermore, the experiments (Yu et al. 2002) showed that the synthesis was insensitive to a range of changes made in the amplitudes and spatial structures assigned to the weights. All of these indicate that the WHOI synthesis was fairly independent of the SOC analysis.

The mean properties of the ECMWF and NCEP2 fluxes and the basic variables are included in the evaluation. Those NWP fluxes are not independent datasets, as the NWP basic meteorological variables are input data in the synthesis though the NWP fluxes are produced by different flux parameterization schemes. The comparisons with the NWP fluxes are made to assess how different the WHOI synthesized flux product is from the NWP flux products and how much the differences come from the improved basic meteorological variables. To make a clear distinction between the biases in the NWP flux schemes and the biases in the NWP basic variables, we have recalculated the NWP fluxes by applying the NWP basic variables to the COARE flux algorithm 2.6a and include them in the comparisons. Therefore, the discrepancies between the WHOI fluxes and the revised NWP fluxes are caused only by the differences in the estimates of flux-related variables. In the following discussions, negative heat fluxes denote the ocean heat loss to the atmosphere and positive heat fluxes denote the ocean heat gain. The presentation starts from the analysis of the flux fields and proceeds onto the analysis of the variable fields.

a. The mean latent and sensible flux fields

Monthly means averaged over the period from 1988 to 1997 are constructed. The 10–yr period is chosen based upon the overlapping time frame between the SOC flux product (1982–97) and the WHOI synthesis (1988–99). The 10-yr averages of the mean latent and sensible flux fields are shown in Figs. 1 and 2, respectively. On each figure, the WHOI synthesized flux fields are compared with the flux fields from the SOC analysis, the ECMWF and NCEP2 outputs, and the revised ECMWF and NCEP fluxes. It can be seen that all six flux products similarly depict the major latent and sensible heat exchange centers. For example, they all have produced large latent heat losses over the region of the Gulf Stream and its extension, major latent heat losses over the broad northern and southern subtropical areas under the influence of the trade winds, large sensible heat losses near the western boundary adjacent to land masses and at high northern latitudes, and weak sensible heat exchanges at mid- and low latitudes. Despite the similarity in structure, the six flux products vary in magnitude. In general, the overall magnitude of the WHOI fluxes is closest to that of the SOC product. Both estimates give the largest net latent heat loss on the order of -175 W m^{-2} and the largest net sensible heat loss on the order of -45 W m^{-2}. Despite the differences in making the two products, the climatological mean aspect of the WHOI fluxes agrees well with that of the SOC fluxes.

The latent and sensible heat fluxes produced from the ECMWF and NCEP2 models are about 25–50 W m^{-2} stronger than the WHOI and SOC estimates over the entire basin. That the NWP fluxes are overestimated has been identified by many studies (e.g., Moyer and Weller 1997; Josey et al. 2001; Smith et al. 2001; Wang and McPhaden 2001; Renfrew et al. 2002; Kubota et al. 2003; Sun et al. 2003). The overestimation is rectified considerably when applying the NWP basic variables to the COARE algorithm 2.6a. The changes are particularly dramatic in the revised NCEP2 latent flux, as the estimation of latent heat loss changes from overestimation to underestimation. For instance, the intensity of the major latent heat loss over the Gulf Stream is reduced from -225 W m^{-2} in the original NCEP2 es-

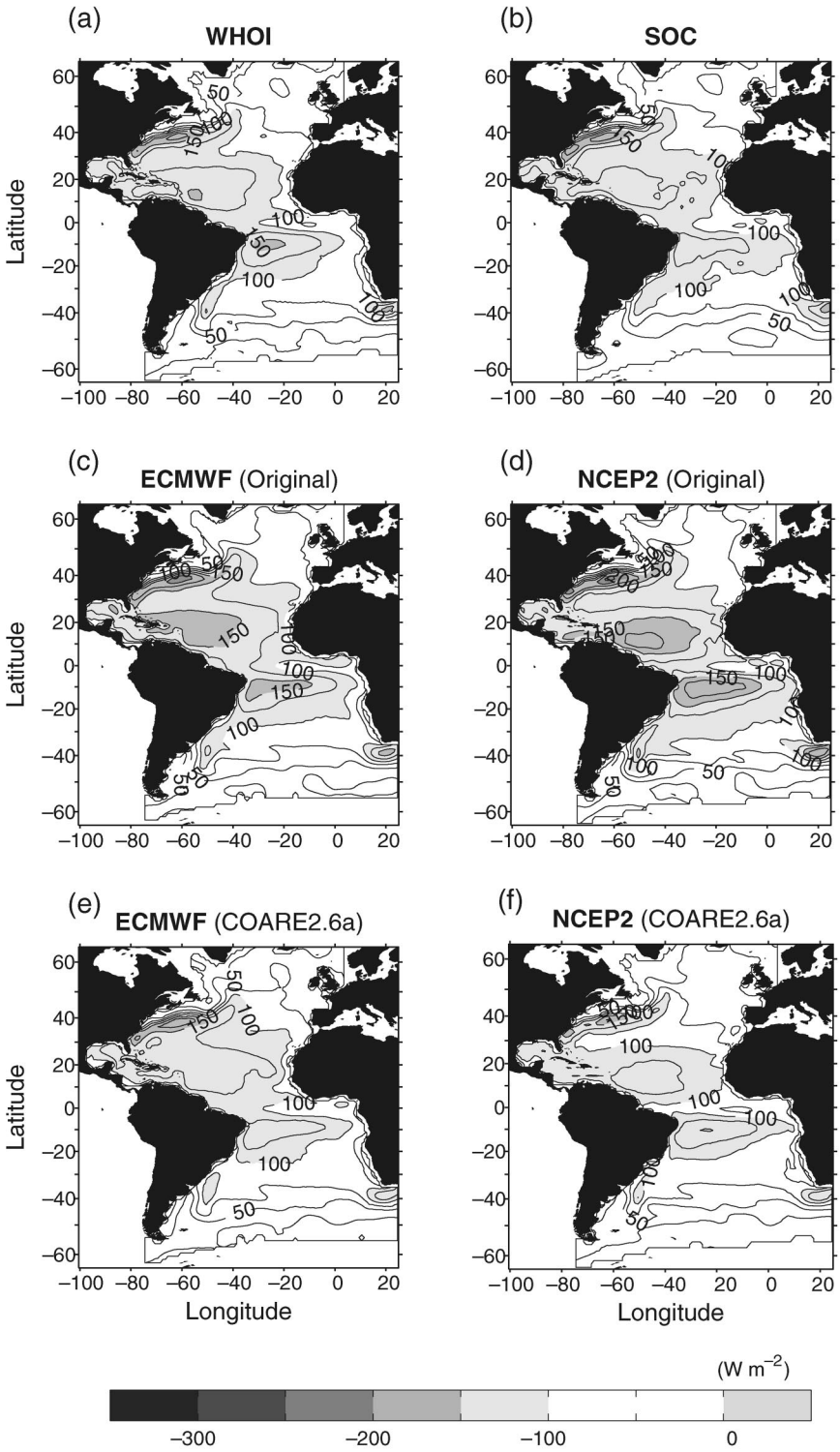

FIG. 1. The 10-yr (1988–97) mean latent heat flux fields from (a) the WHOI analysis, (b) the SOC analysis, (c) the ECMWF operational analysis, (d) the NCEP2 reanalysis, (e) the revised ECMWF flux estimates using the COARE 2.6a flux algorithm, and (f) the revised NCEP2 flux estimates using the COARE flux algorithm 2.6a. Contour interval is 25 W m^{-2}.

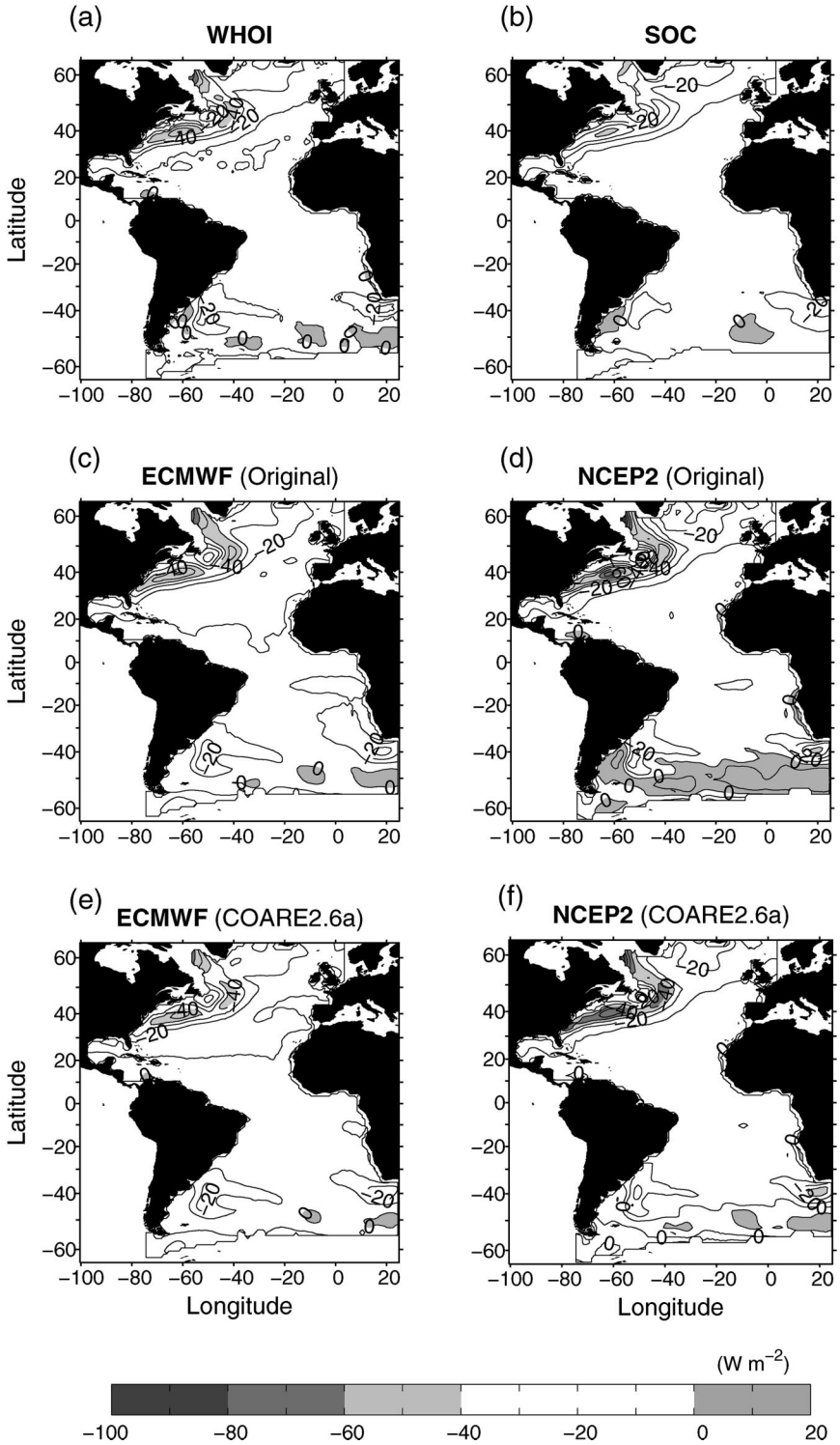

FIG. 2. As in Fig. 1 but for the mean sensible heat flux fields. Contour interval is 10 W m^{-2}.

timation (Fig. 1d) to -150 W m^{-2} in the revised estimation (Fig. 1f). The intensity becomes underestimated by 25 W m^{-2} compared to the WHOI and SOC analysis.

b. The mean turbulent heat flux fields and standard deviations

The pattern of the latent and sensible heat fluxes (Fig. 3) reflects primarily the pattern of the latent flux component except at high northern latitudes where the sensible flux has a significant contribution. The 10-yr average of the standard deviations (STD) of the yearly mean turbulent heat flux fields, which provides a measure of the year-to-year variations of the yearly mean structure, is plotted in Fig. 4. The comparisons show the following features.

- The WHOI STD field (Fig. 4a) is smooth, with relatively large variability occurring over the Gulf Stream, the Labrador Sea, and high southern latitudes. The field's overall structure is similar to that of the NCEP2 (Fig. 4d) and the revised NCEP2 estimation (Fig. 4f).
- The SOC STD field (Fig. 4b) is noisy, particularly in the southern basin where ship data are sparse (Josey et al. 1998). The influence of data distribution on the STD structure is obvious: the flux variability is small along the ship routes, but becomes large away from those routes. Nevertheless, the pattern of the variability in the northern basin between the equator and 45°N is similar among the SOC, WHOI, and both the original and revised NCEP2 fluxes.
- The ECMWF STD field (Fig. 4c) has the largest variability of all the products. The STD for the revised ECMWF fluxes (Fig. 4e) shows that the variability is reduced in the southern and equatorial region and enhanced in the midnorthern basin. However, the STD patterns in both the original and revised versions are very different from the other products. This peculiarity appears to be related to the changing ECMWF operational system (see the data description in section 2b). This problem is to be further discussed in the following section.

c. The change of the mean property with time

To examine the temporal variability of the systematic biases in NWP models, the year-to-year variations of the yearly mean turbulent heat fluxes averaged over the northern Atlantic basin from the equator to 45°N are plotted (Fig. 5). This is the region where the four flux products, that is, the WHOI synthesis, the SOC analysis, and the two versions of NCEP2 fluxes, exhibit similar year-to-year variability (Fig. 4) and the SOC analysis has the better data coverage (Josey et al. 1998). The following interesting features are highlighted in Fig. 5.

- The trend and year-to-year variability of the area-averaged WHOI flux index have the best agreement with those of the SOC index. The time mean deviation is less than 6 W m^{-2} over the 10-yr period from 1988 to 1999. The ECMWF and NCEP2 turbulent fluxes are systematically larger over the entire period. On average, the turbulent heat loss is about 20 W m^{-2} stronger from the ECMWF model and about 18 W m^{-2} stronger from the NCEP2 model.
- The NCEP2 flux index shows a trend of yearly variability consistent with that of the SOC and WHOI fluxes, even though the intensity of the fluxes is persistently larger. The revised NCEP2 fluxes retain the trend, but become persistently weaker.
- The ECMWF index registers a peculiar drop during 1989–92, which is not shown in any other indices. The cause of the drop coincides with the modification made in the moisture transfer coefficients in 1990 for low wind speed and again in 1993 for high wind speed, which increased the latent heat loss by about 20 W m^{-2} in the equatorial region (Siefridt et al. 1999). A modification in the data-handling techniques in December 1994/January 1995 gave a sudden reduction of 10 W m^{-2} at all latitudes. Those changes cause a shift in the mean state. Interestingly, the downward trend during 1989–92 is reversed to the upward trend in the revised ECMWF fluxes. The lack of a steady model platform apparently is the cause of large yearly STD variability in Figs. 4c and 4e.
- The flux algorithms in ECMWF and NCEP2 bias the estimation of the NWP fluxes. The COARE algorithm 2.6a reduces the intensity of the two NWP fluxes. When the intensity of the revised ECMWF fluxes remains stronger than the WHOI fluxes, the intensity of the revised NCEP2 fluxes becomes weaker.
- Though the same flux algorithm is used, there are still considerable differences between the revised NWP fluxes and the WHOI fluxes. The cause of these differences is induced by the differences between the NWP variables and the WHOI variables, which is to be discussed in the next section.

d. The zonally averaged mean fluxes

Zonal averages are constructed for the 10-yr (1988–97) mean latent and sensible heat fluxes. The comparison between the WHOI and SOC products (Fig. 6) shows that the two products agree remarkably well in depicting both magnitude and structure of the zonally averaged latent and sensible heat fluxes. The only major difference between the two products occurs at high southern latitudes. This is not surprising because both datasets contain large uncertainties in this region due to either sparse data or the large uncertainties in the NWP models discussed in section 2d. The comparisons between the WHOI analysis and the two versions of NWP flux estimates are shown in Fig. 7. Consistent with the findings from previous figures, the latent heat loss from

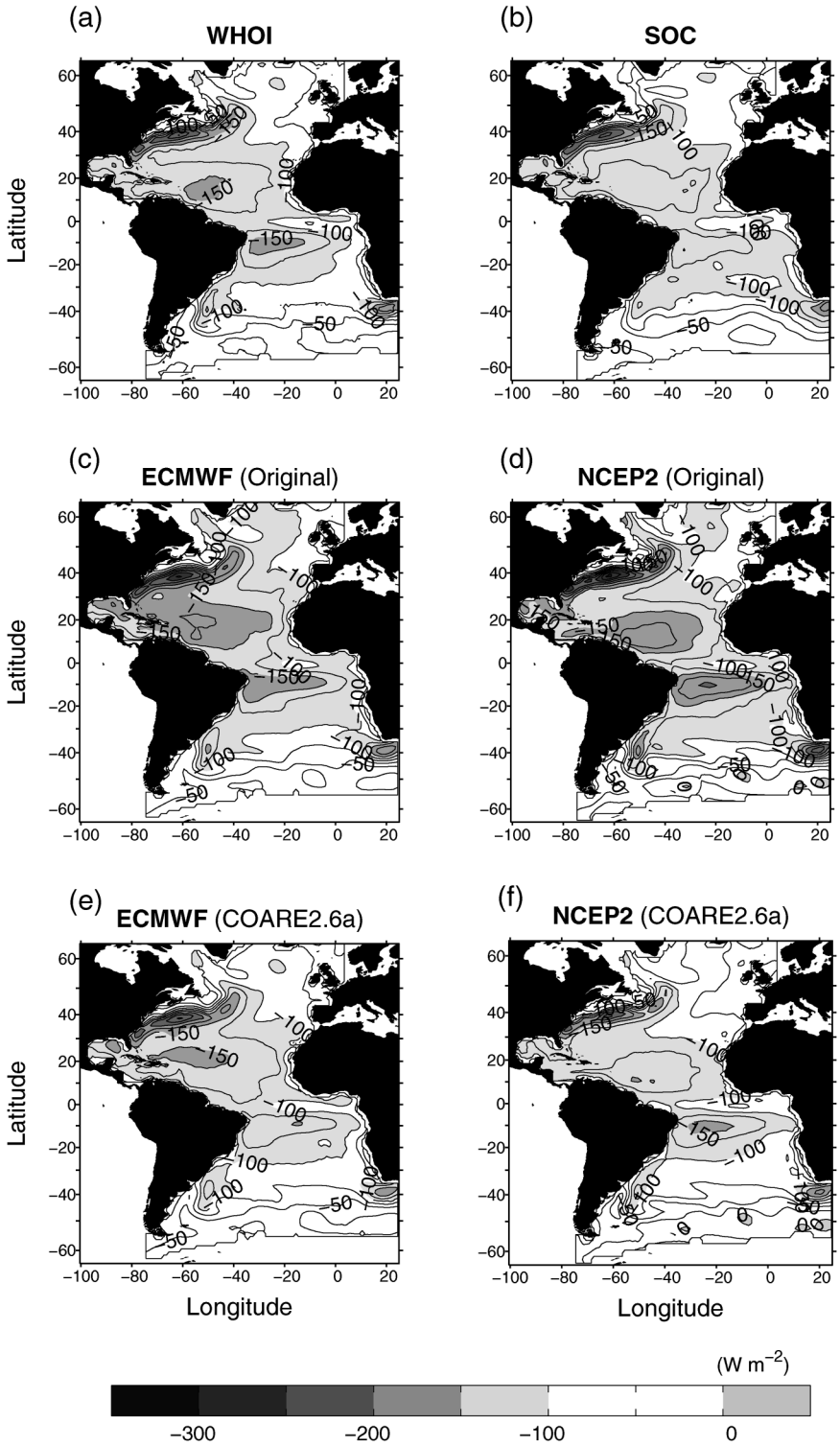

FIG. 3. As in Fig. 1 but for the sum of the mean latent and sensible heat flux fields. Contour interval is 25 W m^{-2}.

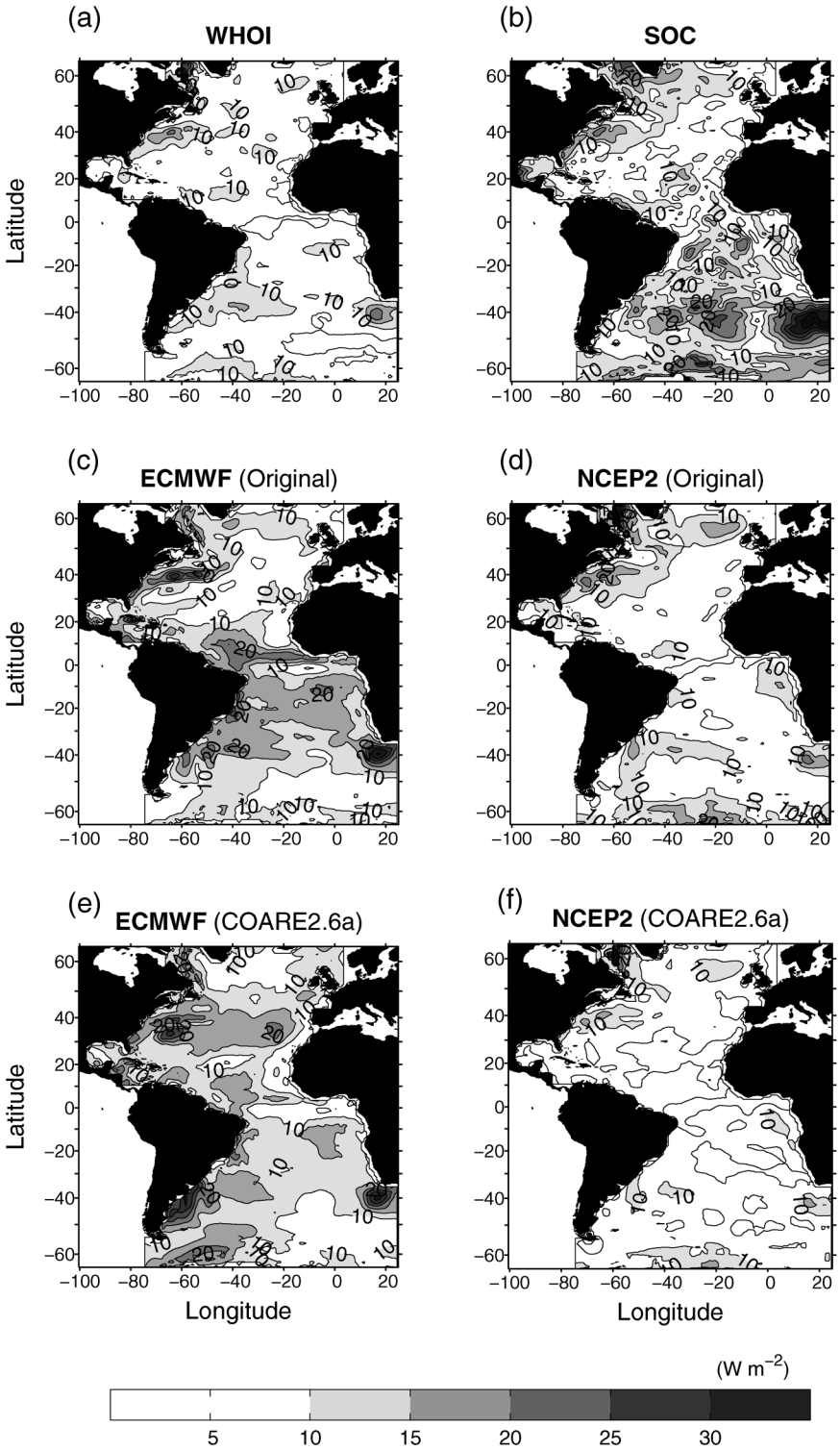

FIG. 4. As in Fig. 1 but for the 10-yr (1988–97) mean std dev of the yearly mean latent and sensible fields. Contour interval is 5 W m^{-2}.

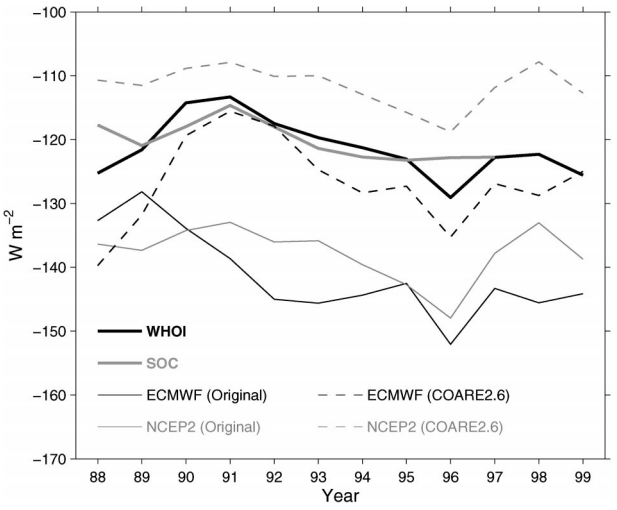

FIG. 5. Comparison of year-to-year variations of the yearly mean latent and sensible heat fluxes produced from the WHOI analysis, the SOC analysis, the ECMWF operational analysis, the NCEP2 reanalysis, and the revised ECMWF and NCEP2 fluxes using the COARE flux algorithm 2.6a. The values are the averages over the North Atlantic basin between the equator and 45°N.

the WHOI analysis is persistently weaker than that of both ECMWF and NCEP2 at all latitudes. The WHOI sensible heat flux is comparable with the NCEP2 in mid- and low latitudes, but is different at higher latitudes. The latter has a sensible heat gain about 10 W m^{-2} near the 50°S. The sensible heat loss from the ECMWF is stronger among all products. The amount of latent and sensible heat loss is much reduced in the revised NWP fluxes. Although the revised ECMWF latent and sensible heat loss is still larger than the respective WHOI value, the revised NCEP2 latent and sensible heat fluxes are both weaker. The direct application of the COARE flux algorithm to the NWP variables did not replicate either the SOC or the WHOI results.

4. Comparisons of flux-related basic variables

The latent and sensible heat fluxes are predominantly determined by a combination of wind speed (U) and sea–air humidity and temperature gradients [($q_s - q_a$) and ($T_s - T_a$)]. The relationship between the fluxes and the flux-related variables is highly nonlinear as the turbulent exchange coefficients [Eqs. (1)–(2)] are also a function of wind speed and stability (Liu et al. 1979; Fairall et al. 1996; Bradley et al. 2000). Here we examine the characteristics and temporal changes of mean variable properties estimated from the synthesis by comparing them with those of the SOC and NWP variables. Three sets of plots are made, which include variations of yearly mean indices of the flux-related basic variables and the sea–air humidity and temperature gradients averaged over the northern Atlantic basin between the equator and 45°N (Fig. 8), variations of the variable combinations $-U(q_s - q_a)$ and $-U(T_s - T_a)$ (Fig. 9), and zonally averaged 10-yr mean quantities (Fig. 10). In Fig. 8, satellite retrievals of wind speed, air specific humidity, and surface temperature are superimposed. This can help to assess the influence of satellite data on the estimation of variables. Major characteristics are summarized as follows.

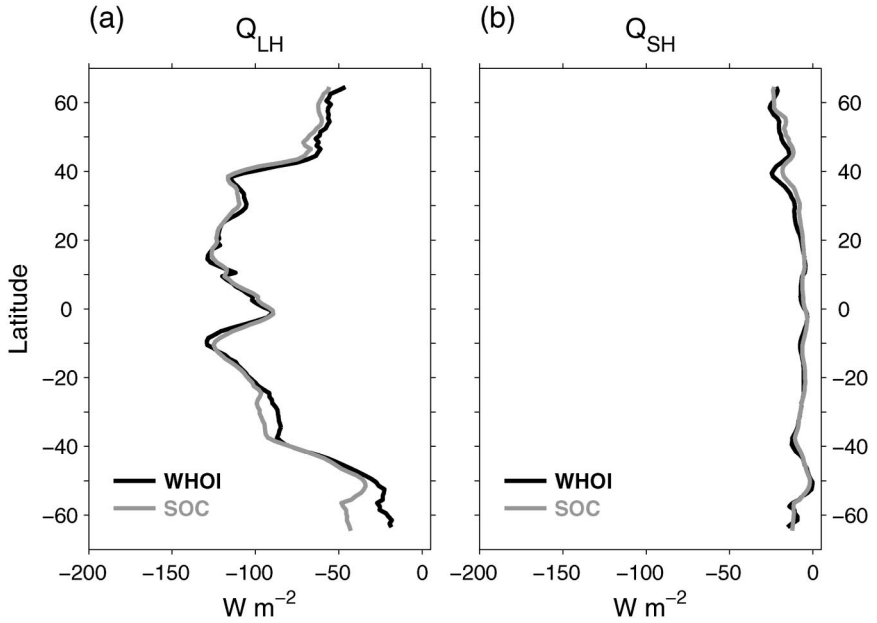

FIG. 6. Comparison of the zonal averages of the 10-yr (1988–97) mean (a) latent and (b) sensible heat flux from the WHOI analysis and the SOC climatology.

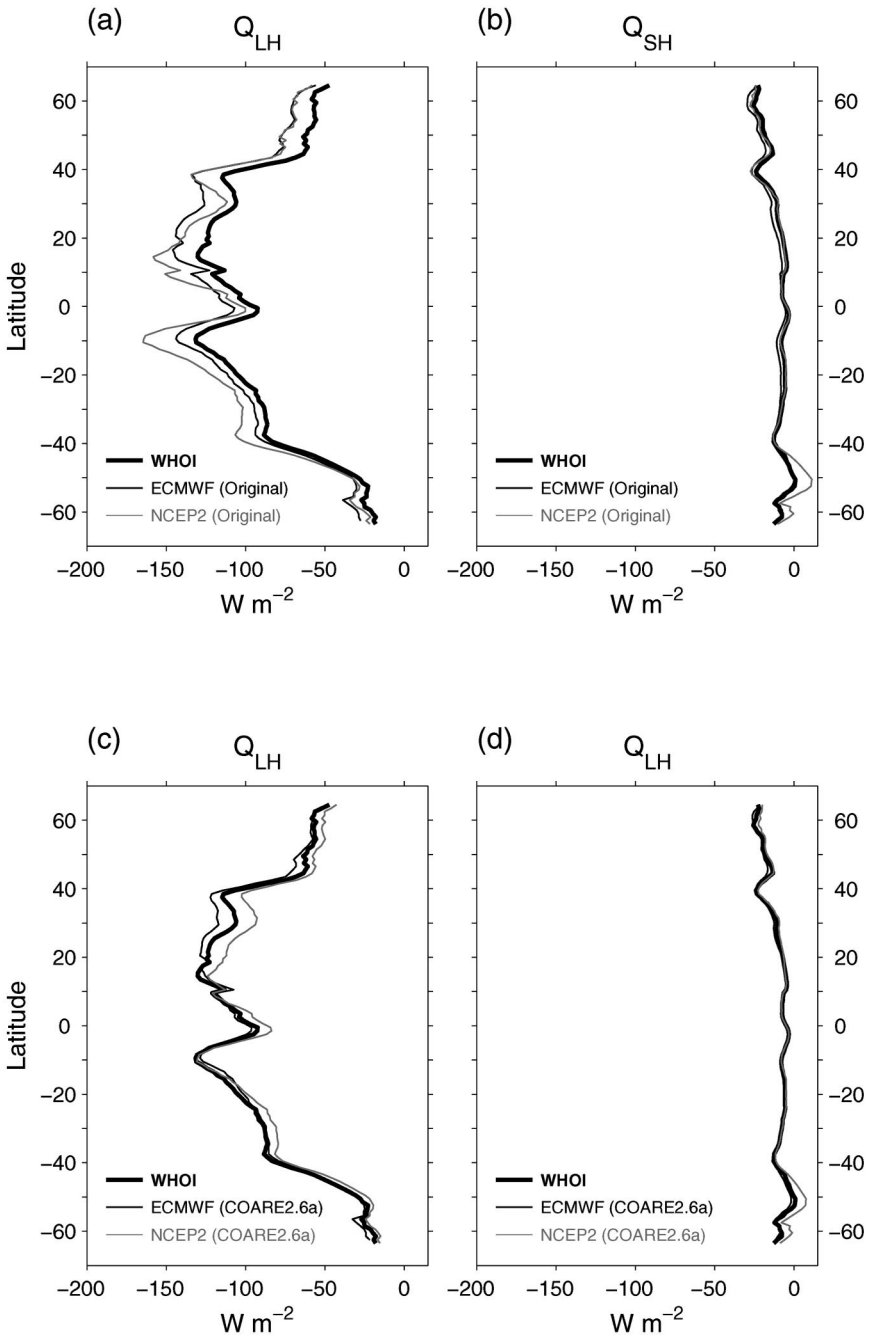

FIG. 7. Comparison of zonal averages of the 10-yr (1988–97) mean (a) latent and (b) sensible heat fluxes from the WHOI analysis, the ECMWF and NCEP2 outputs, and (c) latent and (d) sensible heat fluxes from the WHOI analysis, the revised ECMWF and NCEP fluxes using the COARE flux algorithm 2.6a.

a. Comparison with the SOC climatology

Although the yearly mean WHOI fluxes agree well with the mean SOC fluxes (Figs. 5–6), the yearly mean variables from the two products are different and the differences are persistent over the period 1988–95 (Fig. 8, note that the SOC variables are available to us only up to 1995 although the SOC fluxes are up to 1997). The SOC product has greater wind speed, wetter air at 2 m and cooler sea surface and 2-m air temperatures.

b. Comparison with the NWP model outputs

The variables estimated from the WHOI synthesis are clearly different from the NWP outputs. The wind speed

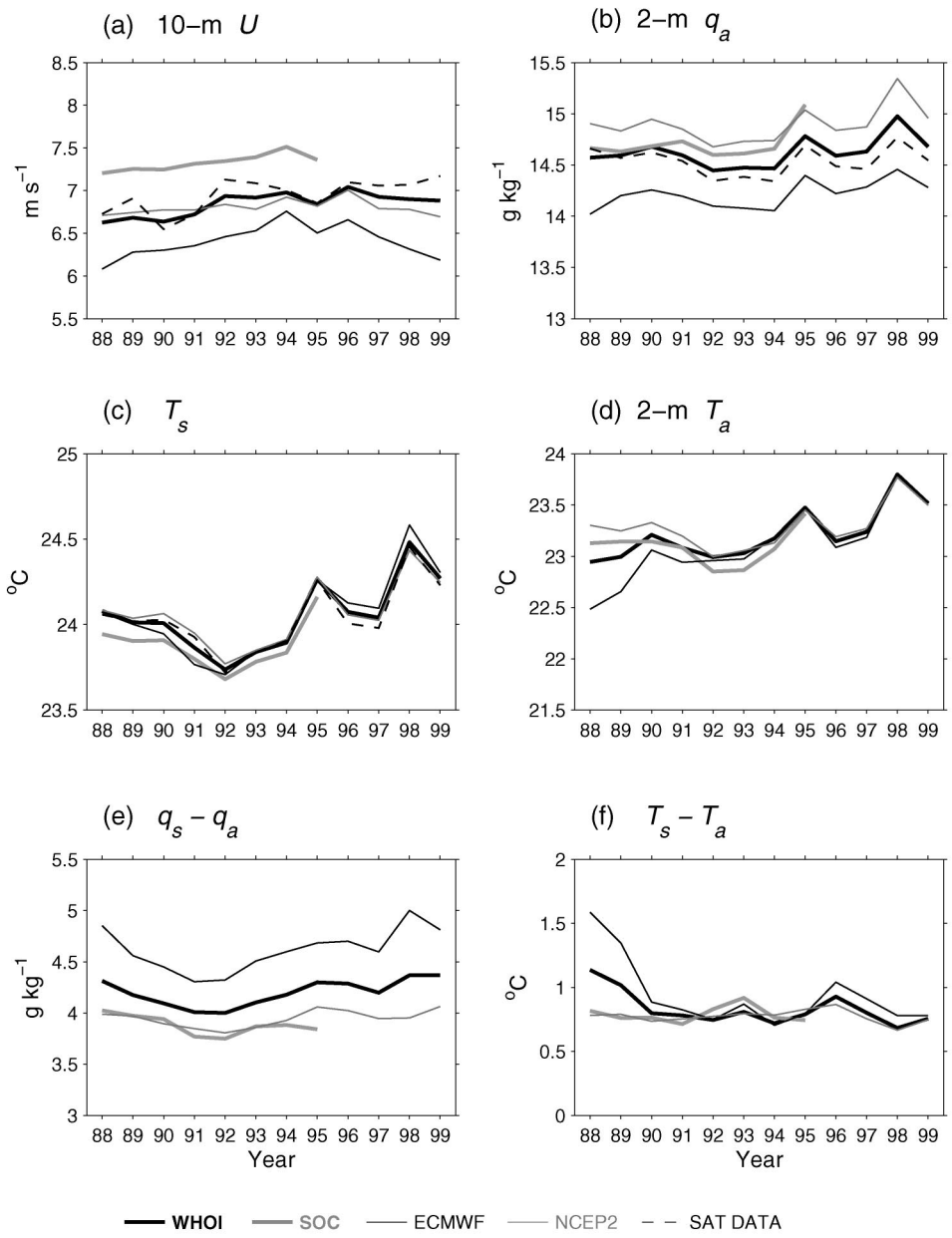

FIG. 8. Comparison of year-to-year variations of the yearly mean (a) 10-m wind speed, (b) 2-m air humidity, (c) sea surface temperature, (d) 2-m air temperature, (e) sea–air humidity gradient, and (f) sea–air temperature gradient. The values are the averages over the northern Atlantic basin between the equator and 45°N.

is about 0.5 m s^{-1} stronger than ECMWF but is only slightly larger than NCEP2 after 1992. The 2-m air is wetter than in ECMWF but drier than in NCEP2 and the differences persist over the entire synthesis period. The 2-m air temperature is very similar to both NCEP2 and ECMWF after 1992 but is colder than in NCEP2 and warmer than in ECMWF before 1992. The differences in the surface temperature are small; the estimates from all of the products are quite similar.

Only in the 2-m air temperature index is the increase of 0.5°C during the period of 1988–91 noticeably incoherent with NCEP2 and SOC. In general, the tendency of year-to-year variations of the ECMWF variables is similar to those from NCEP2, SOC, and satellites, despite constant modifications made to the ECMWF operational forecast/analysis model (see section 2b). This is in sharp contrast with the ECMWF flux estimates, which are more susceptible to the model updates (Fig. 5).

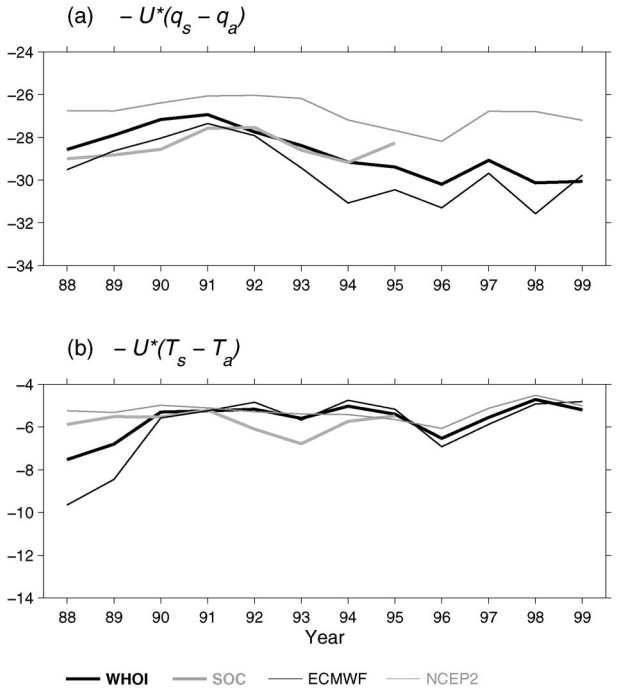

FIG. 9. Comparison of year-to-year variations of the yearly mean (a) $-U(q_s - q_a)$ and (b) $-U(T_s - T_a)$. Negative signs are added to be consistent with the sign in Fig. 5. The values are the averages over the northern Atlantic basin between the equator and 45°N.

c. Comparison with satellite data

The WHOI wind speed is slightly weaker than the SSM/I-derived wind speed, but it best replicates the satellite data among all products (Fig. 8a). The 2-m air humidity is persistently wetter than the SSM/I humidity (Fig. 8b), but its difference with the satellite data is smallest among all products. The surface temperatures from all products, except the SOC, are very similar. There are no satellite observations of air temperature in the synthesis.

The synthesis cancels out the errors in input data and produces an optimal estimate that has the minimum error variance. It is expected that the variable estimates from the synthesis should have better accuracy than the NWP data. Therefore, it is not surprising to see the better agreement between the synthesized variables and the satellite data. However, the satellite data cannot be used to verify the improvement in the WHOI variables over the NWP outputs due to their inclusion in the synthesis. Such an assessment has to be conducted with in situ flux buoy measurements that are high quality, and also kept from the WHOI synthesis and the NWP assimilations (YSW).

d. Comparison of variable combinations

Although the wind speed and sea–air humidity and temperature gradients estimated from the WHOI and SOC products have considerable differences (Fig. 8), the deviations in the variable combinations, $-U(q_s - q_a)$ and $-U(T_s - T_a)$, are smaller and less systematic (Fig. 9, note that negative signs are added to be consistent with the signs of latent and sensible heat fluxes in Fig. 5). Obviously, the differences are compensated when the variables are combined, resulting in a much better agreement between the combined products.

Studies have shown that the air humidity products from the two NWP models have different biases. The ECMWF has drier air (Klinker 1997) while the NCEP2 has wetter air (Sun et al. 2003). This is particularly evident for the tropical oceans. The estimates of air humidity from the WHOI synthesis appear to represent a degree of improvement (Fig. 8b). It appears that the biases in the NWP air humidity are the major source of error in the flux estimates. It can be seen that, despite the compensation effect, the differences in $-U(q_s - q_a)$ reflect largely the differences in the 2-m air humidity rather than the differences in wind speed. Similarly, the differences in $-U(T_s - T_a)$, particularly during the period of 1988–91, reflect predominantly the differences in the 2-m air temperature.

In general, the trend and year-to-year variations of $-U(q_s - q_a)$ are consistent with those of the latent flux estimates (Fig. 5). This quantity agrees better with the revised NWP fluxes using the COARE algorithm 2.6a (i.e., the two dashed lines in Fig. 5) rather than the fluxes from the NWP outputs. Understandably, changes in the model parameterizations have more impact on the flux estimates, while less on the flux-related variables. The fluxes are the by-product of the forecast model and do not directly impact the model forecast. The purpose of the model upgrade is to improve the representation of the basic variables for better weather forecasts. Sometimes such improvement may be at the expense of the flux estimation.

e. Comparison of zonally averaged quantities

The comparison of the 10-yr (1988–97) mean, zonally averaged quantities (wind speed, sea–air humidity, and temperature gradients, and their multiplications) with the NWP results is shown in Fig. 10. The comparison with the SOC climatology is presented in Fig. 11, but the values are averaged over a shorter period from 1988 to 1995 because of the limited availability of the SOC-analyzed basic variables. Some characteristics of the variable differences between the WHOI analysis, the SOC climatology, and the NWP models are similar to Fig. 8, though the latter was constructed for the region (0°, 45°N).

1) COMPARISON WITH NWP OUTPUTS

The major features in Fig. 10 are summarized as follows.

- The WHOI wind speed has good agreement with

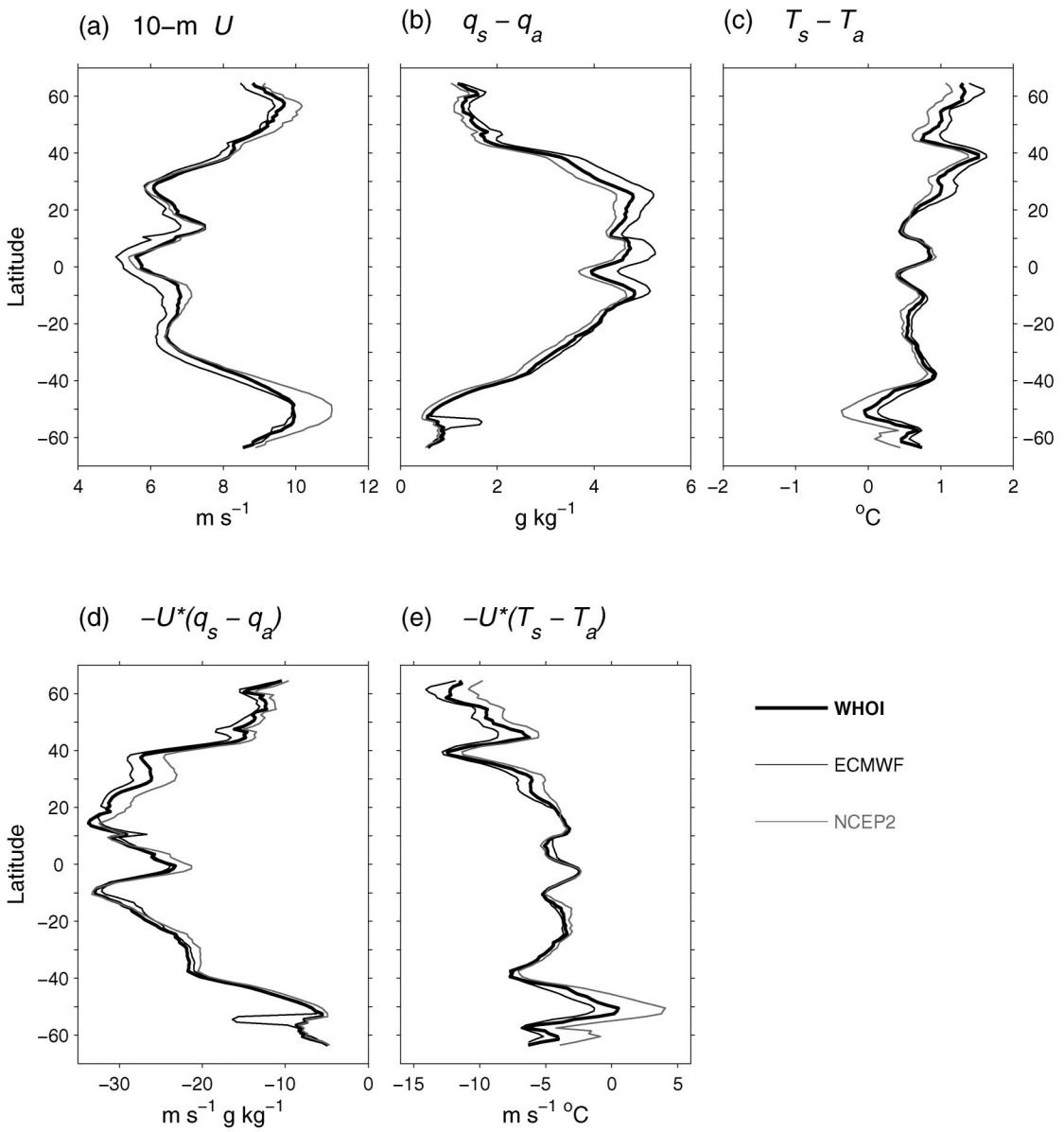

FIG. 10. Comparison of zonal averages of the 10-yr (1988–97) mean of (a) wind speed, (b) sea–air humidity gradient, (c) sea–air temperature gradient, (d) $-U(q_s - q_a)$, and (e) $-U(T_s - T_a)$ between the WHOI analysis and the NWP models.

NCEP2 at mid- and low latitudes between 40°S and 40°N, while it is weaker than NCEP2 at high latitudes poleward of 40°. On the other hand, the WHOI wind speed is stronger than ECMWF at all latitudes.

- The WHOI sea–air humidity gradient is weaker than ECMWF and stronger than NCEP2 at all latitudes. Similarly, the WHOI sea–air temperature gradient is also weaker than ECMWF and NCEP2 although the differences are small in the region between 40°S and 15°N.
- The effects of error compensation are clearly at work, as the differences in the variable combinations, $-U(q_s - q_a)$ and $-U(T_s - T_a)$, from different products are not as persistent as the differences in U. The differences in $-U(q_s - q_a)$ are smaller at the southern latitudes between 45° and 5°S but larger at the northern latitudes from the equator to 60°N. The differences in $-U(T_s - T_a)$ are largest at high latitudes (poleward of ~40°).
- The structure of the differences in $-U(q_s - q_a)$ and $-U(T_s - T_a)$ is similar to that in the latent and sensible heat fluxes that were calculated from the COARE flux algorithm 2.6a (Figs. 7c–d); however, it cannot be related to that in the fluxes from the ECMWF and NCEP2 models (Figs. 7a–b). Apparently, the ECMWF and NCEP2 flux algorithms are biased.

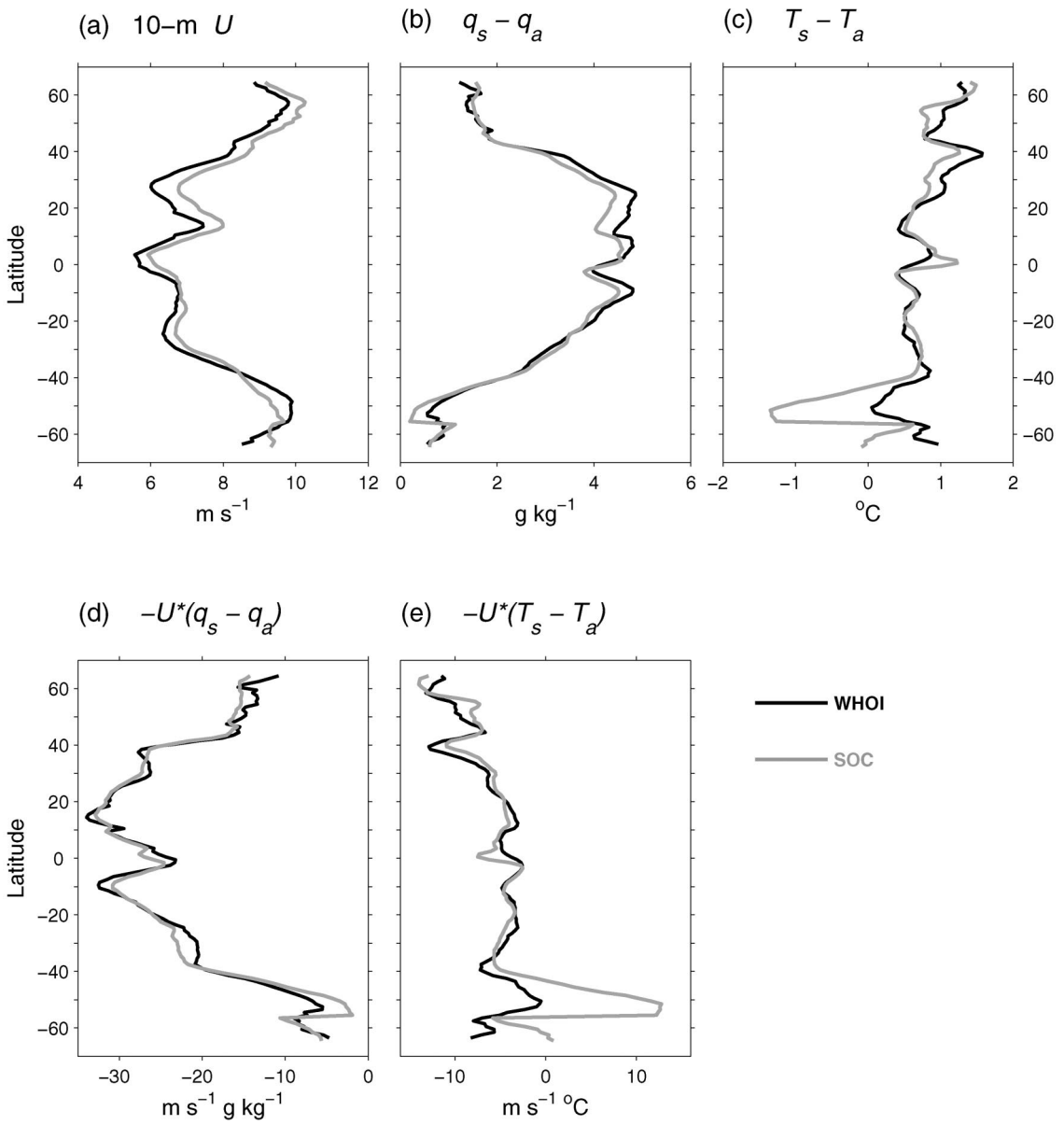

FIG. 11. Comparison of zonal averages of the 8-yr (1988–95) mean of (a) wind speed, (b) sea–air humidity gradient, (c) sea–air temperature gradient, (d) $-U(q_s - q_a)$, and (e) $-U(T_s - T_a)$ between the WHOI analysis and the SOC data.

2) COMPARISON WITH THE SOC CLIMATOLOGY

The major features in Fig. 11 are as follows:

- In comparison with the SOC results, the WHOI wind speed is weaker at all latitudes, the sea–air humidity gradient is larger at latitudes between 20°S and 40°N, and the sea–air temperature gradient is larger at latitudes northward of 20°N and also southward of 35°S. The difference between the two products in the sea–air temperature gradient is very large (>1°C) at latitudes around 50°S.
- The two products have better agreement in the variable combinations, $-U(q_s - q_a)$ and $-U(T_s - T_a)$, than in either individual component. The effects of error compensation are apparent, as the differences in $-U(q_s - q_a)$ are small at mid- and low latitudes, despite the considerable differences in U and $(q_s - q_a)$.
- In comparison with Fig. 6, the WHOI and SOC products agree well in the fluxes but not necessarily in the individual variables.

5. Summary and discussion

A new daily latent and sensible flux product developed at WHOI with 1° × 1° resolution for the Atlantic Ocean (65°S to 65°N) for the period from 1988 to 1999

was presented. The flux product was developed by using a variational objective analysis approach to obtain best estimates of the flux-related basic surface meteorological variables (e.g., wind speed, air humidity, air temperature, and sea surface temperature) through synthesizing satellite and NWP data. The state-of-the-art COARE bulk flux algorithm 2.6a was applied to compute the flux fields. The retrievals of the SSM/I wind speed and air humidity and AVHRR sea surface temperature and the outputs of the ECMWF operational forecast model and NCEP2 reanalysis–forecast model were included in the synthesis.

The variational objective analysis involves a direct minimization of an objective function that consists of a number of terms, each measuring the departure of the analysis field from input data fields. Associated with each term is a weight, which is inversely proportional to the error covariance of input data field and needs to be prescribed. The weights used in the study were constants, fine-tuned with in situ buoy measurements. Sensitivity experiments (Yu et al. 2002) have found that the quality of the input data is a key factor that determines the degree of sensitivity of the solution fields to the weights. In the regions north of 40°S, the influence of the weights on the solution fields is small and the errors in the flux estimates induced by the weights do not exceed 3 W m^{-2} in the latent flux fields and 0.5 W m^{-2} in the sensible flux fields. However, caution should be exercised in interpreting the fluxes south of 40°S.

The WHOI fluxes have daily resolution. Their characteristics at daily time scales are analyzed in a companion paper (Yu et al. 2003) that used benchmark time series provided by data from in situ flux buoys as verification. This study focused on analyzing the mean field structures and properties of the daily flux fields over the period of 1988–97 through comparisons with the SOC climatology and the NCEP2 and ECMWF model outputs. The analysis period is 2 yr shorter than the synthesis period (1988–99) because the SOC analysis is available only up to 1997. The SOC climatology was based upon ship meteorological reports from COADS, a data source independent from the WHOI synthesis. Therefore, the SOC climatology is a useful source for comparison, though the climatology was constructed with many approximations and has considerable degrees of uncertainties (Josey et al. 1999). On the other hand, the NWP fluxes are not independent of the WHOI fluxes as the flux-related variables from the NWP models were included in the synthesis. The comparison was to assess how different the synthesized WHOI fluxes are from the NWP fluxes and how much the differences are related to the differences in the flux-related variables. The differences in the flux estimates are attributable to both differences in the estimates of the flux-related variables and the differences in the flux bulk algorithms. To make a clear distinction between the two types of differences, the COARE flux algorithm 2.6a was used with the NWP flux-related variables to recalculate the fluxes. The revised NWP fluxes were included as additional information in the comparison. Major findings from the comparison analysis are summarized as follows:

- The comparison with the SOC climatology shows that the two products agree well in the mean values of the fluxes: both the mean field structures and the year-to-year variations are similar in pattern and amplitude. However, the two products do not necessarily agree in the mean values of the flux-related variables: the WHOI synthesis yielded a weaker wind speed at all latitudes and a stronger sea air humidity gradient at mid- and low latitudes. It is found that the better agreement in the fluxes is due to the effects of error compensation during variable combinations.
- The WHOI fluxes agree well with the NCEP2 reanalysis fluxes in structure and the trend of year-to-year variations but not in amplitude. On average, the NCEP2 turbulent (latent and sensible) heat loss is about 18 W m^{-2} stronger. The WHOI wind speed is very close to the NCEP2 wind at mid- and low latitudes, but is slightly weaker at high latitudes. Both sea–air humidity and temperature gradients are, however, slightly larger than NCEP2.
- The ECMWF fluxes are about 20 W m^{-2} stronger on average. The comparison of the year-to-year variations was not good due to changes related to the modifications introduced in the ECMWF operational models. Among the numerous changes made during the synthesis period, there were a few that had major impacts on the flux estimates. The increased latent heat loss by about 20 W m^{-2} during 1989–92 corresponded to the changes in the moisture transfer coefficients in 1990 for low wind speed and again in 1993 for high wind speed (Siefridt et al. 1999). A modification in data-handling techniques in December 1994–January 1995 gave a sudden reduction of 10 W m^{-2} at all latitudes. Those changes in the model caused a distortion in the mean state and resulted in large yearly STD variability in the ECMWF fluxes. Interestingly, the degree of changes in the flux-related variables induced by the model upgrades was not as dramatic as the fluxes. Only the 2-m air temperature field is found to have a suspiciously large increase during 1988–90. The trend of year-to-year variations for other variables agrees reasonably well with other products. This justifies the inclusion of the basic variables, not the fluxes, from the ECMWF operational model in the synthesis.
- The flux algorithms in both NWP models bias the flux estimation. The revised NWP fluxes that used the COARE flux algorithm 2.6a reduce the turbulent heat loss considerably. The revised ECMWF fluxes are still stronger than WHOI, but the downward trend observed between 1989 and 1992 is reversed to an upward trend. The revised NCEP2 fluxes are, however, much weaker than WHOI. All of these point out that

the direct application of the COARE algorithm did not replicate the WHOI results.
- The flux-related variables from the WHOI synthesis are closest to the input satellite observations (wind speed, humidity, surface temperature). However, the satellite data cannot be used to verify the improvement in the WHOI variables over the NWP outputs due to their inclusion in the synthesis. Such an assessment has to be done with in situ flux buoy measurements that are high quality and are also kept from the WHOI synthesis and the NWP assimilations.

The synthesis cancels out the errors in input data and produces an optimal estimate that has the minimum error variance. It is expected that the variable estimates from the synthesis should have better accuracy than the NWP outputs. Therefore, the fluxes produced by using the best estimates of basic variables and the state-of-the-art COARE algorithm should represent an improvement over the NWP fluxes. Indeed, our recent validation analysis (Yu et al. 2003) based upon daily in situ measurements acquired from flux buoys and ships showed that the WHOI variables have good agreement with the measurements and the WHOI fluxes are an improvement over the NWP fluxes at all measurement sites.

The availability of satellite and NWP model data is ever increasing. Each type of data source has different advantages and disadvantages in terms of spatial coverage, temporal and spatial resolutions, and comes with different instrumental/model biases. The differences influence both accuracy and temporal and spatial representativeness of the flux estimates that are constructed from each of these data sources. There is a need to develop innovative approaches to take advantage of existing data sources and obtain a field that is more representative and accurate. This study is the first to demonstrate that the synthesis approach is a useful tool for combining the NWP and satellite data sources and improving the mean representativeness of the basic variable fields and, thus, the flux fields. It is anticipated that the synthesis approach may become increasingly relied upon in the preparation of future flux products.

Acknowledgments. This work is supported by the NOAA CLIVAR Atlantic program under Grant NA06GP0453. The authors would like to acknowledge Frank Wentz and the Remote Sensing Systems Company for providing the SSM/I wind speed product, Shu-Hsien Chou and the surface turbulent fluxes research group at NASA GSFC (Code 912) for the humidity retrievals from version 2 of Goddard Satellite-Based Surface Turbulent Fluxes (GSSTF) product, the JPL PODACC (Physical Oceanography Distributed Active Archive Center), for the NOAA–NASA AVHRR Oceans Pathfinder sea surface temperature data, and the Data Support Section at NCAR for the ECMWF and NCEP2 data. We thank Simon Josey for his generosity in providing the monthly SOC data from 1982 to 1997 for our analysis. We are also grateful to Simon Josey, Terry Joyce, and an anonymous reviewer for their valuable comments on the manuscript. Ms. Barbara Gaffron read and edited the manuscript.

REFERENCES

Atlas, R., R. N. Hoffman, and S. C. Bloom, 1993: Surface wind velocities over the ocean. *Atlas of Satellite Observations Related to Global Change*, R. J. Gurney, J. L. Foster, and C. L. Parkinson, Eds., Cambridge University Press, 128–139.

Beljaars, A. C. M., 1997: Air–sea interaction in the ECMWF model. *Proc. Seminar on Atmosphere–Surface Interaction*, Reading, United Kingdom, ECMWF, 33–52.

Bradley, E. F., C. W. Fairall, J. E. Hare, and A. A. Grachev, 2000: An old and improved bulk algorithm for air–sea fluxes: COARE2.6a. Preprints, *14th Symp. on Boundary Layer and Turbulence*, Aspen, CO, Amer. Meteor. Soc., 294–297.

Bretherton, F. P., R. E. Davis, and C. B. Fandry, 1976: A technique for objective analysis and design of an oceanographic experiment applied to MODE-73. *Deep-Sea Res.*, **23,** 559–582.

Brown, J. W., O. B. Brown, and R. H. Evans, 1993: Calibration of AVHRR infared channels: A new approach to non-linear correction. *J. Geophys. Res.*, **98,** 18 257–18 268.

Brunke, M. A., C. W. Fairall, X. Zeng, L. Eymard, and J. A. Curry, 2003: Which bulk aerodynamic algorithms are least problematic in computing ocean surface turbulent fluxes? *J. Climate*, **16,** 619–635.

Bunker, A. F., 1976: Computations of surface energy flux and annual air–sea interaction cycles of the North Atlantic Ocean. *Mon. Wea. Rev.*, **104,** 1122–1140.

Chou, S.-H., R. M. Atlas, C.-L. Shie, and J. Ardizzone, 1995: Estimates of surface humidity and latent heat fluxes over oceans from SSM/I data. *Mon. Wea. Rev.*, **123,** 2405–2425.

——, C.-L. Shie, R. M. Atlas, and J. Ardizzone, 1997: Air–sea fluxes retrieved from Special Sensor Microwave Image data. *J. Geophys. Res.*, **102,** 12 705–12 726.

——, E. J. Nelkin, J. Ardizzone, R. M. Atlas, and C.-L. Shie, 2003: Surface turbulent heat and momentum fluxes over global oceans based on the Goddard satellite retreivals, version 2 (GSSTF2). *J. Climate*, **16,** 3256–3273.

Curry, J. A., C. A. Clayson, W. B. Rossow, R. Reeder, Y. C. Zhang, P. J. Webster, G. Liu, and R. S. Sheu, 1999: High-resolution satellite-derived dataset of the ocean surface fluxes of heat, freshwater and momentum for the TOGA COARE IOP. *Bull. Amer. Meteor. Soc.*, **80,** 2059–2080.

Daley, R., 1991: *Atmospheric Data Analysis*. Cambridge University Press, 457 pp.

da Silva, A. M., C. C. Young, and S. Levitus, 1994: *Anomalies of Heat and Momentum Fluxes, Atlas of Surface Marine Data*, NOAA Atlas NESDIS 8, 413 pp.

ECMWF, 1994: The description of the ECMWF/WCRP level III—A atmospheric data archive. ECMWF Tech. Attachment, 72 pp.

Esbensen, S. K., and Y. Kushnir, 1981: Heat budget of the global ocean: Estimates from surface marine observations. Climate Research Institute, Oregon State University Tech. Rep. 29, 271 pp.

Fairall, C. W., E. F. Bradley, D. P. Rogers, J. B. Edson, and G. S. Young, 1996: Bulk parameterization of air–sea fluxes for TOGA COARE. *J. Geophys. Res.*, **101,** 3747–3764.

——, ——, J. E. Hare, A. A. Grachev, and J. B. Edson, 2003: Bulk parameterization of air–sea fluxes: Updates and verification for the COARE algorithm. *J. Climate*, **16,** 571–591.

Gandin, L. S., 1963: *Objective Analysis of Meteorological Fields.* Hydrometeozidat, 236 pp.

Gleckler, P. J., and B. C. Weare, 1997: Uncertainties in global ocean surface heat flux climatologies derived from ship observations. *J. Climate*, **10,** 2764–2781.

Halpern, D., V. Zlotnicki, J. Newman, O. Brown, and F. Wentz, 1994: An atlas of monthly distributions of GEOSAT sea surface height,

SSMI surface wind speed, AVHRR/2 sea surface temperature, and ECMWF surface wind components during 1988. Jet Propulsion Laboratory Publication 91-8, 110 pp.

Hsiung, J., 1986: Mean surface energy fluxes over the global ocean. *J. Geophys. Res.,* **91,** 10 585–10 606.

Isemer, H. J., and L. Hasse, 1985: *Observations.* Vol. 1, *Bunker Climate Atlas of the North Atlantic Ocean*, Springer-Verlag, 218 pp.

——, and ——, 1987: *Bunker Climate Atlas of the North Atlantic Ocean, Air–Sea Interactions.* Springer-Verlag, 252 pp.

Jones, C. S., D. M. Legler, and J. J. O'Brien, 1995: Variability of surface fluxes over the Indian Ocean: 1960–1989. *Global Atmos. Ocean Syst.,* **3,** 3249–3272.

Josey, S. A., 2001: A comparison of ECMWF, NCEP–NCAR, and SOC surface heat fluxes with moored buoy measurements in the subduction region of the northeast Atlantic. *J. Climate,* **14,** 1780–1789.

——, E. C. Kent, and P. K. Taylor, 1998: The Southampton Oceanography Centre (SOC) ocean-atmosphere heat, momentum and freshwater flux atlas. Southampton Oceanography Centre Rep. 6, 30 pp.

——, ——, and ——, 1999: New insights into the ocean heat budget closure problem from analysis of the SOC air–sea flux climatology. *J. Climate,* **12,** 2685–2718.

Kalnay, E., and Coauthors, 1996: The NCEP/NCAR 40-Year Reanalysis Project. *Bull. Amer. Meteor. Soc.,* **77,** 437–471.

Kanamitsu, M., 1989: Description of the NMC global data assimilation and forecast system. *Wea. Forecasting,* **4,** 334–342.

——, W. Ebisuzaki, J. Woolen, J. Potter, and M. Fiorion, 2000: An overview of NCEP/DOE Reanalysis-2. *Proc. 2nd Int. Conf. on Reanalyses,* Reading, United Kingdom, WMO, 1–4.

Klinker, E., 1997: Diagnosis of the ECMWF model performance over the tropical oceans. *Proc. Seminar on Atmosphere–Surface Interaction,* Reading, United Kingdom, ECMWF, 53–66.

Kubota, M., A. Kano, H. Muramatsu, and H. Tomita, 2003: Intercomparison of various surface latent heat flux fields. *J. Climate,* **16,** 670–678.

Legler, D. M., I. M. Navon, and J. J. O'Brien, 1989: Objective analysis of pseudostress over the Indian Ocean using a direct-minimization approach. *Mon. Wea. Rev.,* **117,** 709–720.

Liu, W. T., K. B. Katsaros, and J. A. Businger, 1979: Bulk parameterizations of air–sea exchanges of heat and water vapor including molecular constraints at the interface. *J. Atmos. Sci.,* **36,** 1722–1735.

McClain, E. P., W. G. Pichel, and C. C. Walton, 1985: Comparative performance of AVHRR-based multichannel sea surface temperatures. *J. Geophys. Res.,* **90,** 11 587–11 601.

Moyer, K. A., and R. A. Weller, 1997: Observations of surface forcing from the Subduction Experiment: A comparison with global model products and climatological datasets. *J. Climate,* **10,** 2725–2742.

Oberhuber, J. M., 1988: An atlas based on the 'COADS' data set: The budgets of heat, buoyancy and turbulent kinetic energy at the surface of the global ocean. Max-Planck-Institut für Meteorologie Rep. 15, 20 pp.

Rabier, F., J.-N. Thépaut, and P. Courtier, 1998: Extended assimilation and forecast experiments with a four-dimensional variational assimilation system. *Quart. J. Roy. Meteor. Soc.,* **124,** 1861–1887.

Renfrew, I. A., G. W. K. Moore, P. S. Guest, and K. Bumke, 2002: A comparison of surface layer and surface turbulent flux observations over the Labrador Sea with ECMWF analyses and NCEP reanalyses. *J. Phys. Oceanogr.,* **32,** 383–400.

Reynolds, R. W., and T. M. Smith, 1994: Improved global sea surface temperature analyses using optimum interpolation. *J. Climate,* **7,** 929–948.

Schulz, J., P. Schlüssel, and H. Graßl, 1993: Water vapor in the atmospheric boundary layer over oceans from SSM/I measurements. *Int. J. Remote Sens.,* **14,** 2773–2789.

——, J. Meywerk, S. Ewald, and P. Schlüssel, 1997: Evaluation of satellite-derived latent heat fluxes. *J. Climate,* **10,** 2782–2795.

Siefridt, L., B. Barnier, K. Beranger, and H. Roquet, 1999: Evaluation of operational ECMWF surface heat fluxes: Impact of parameterization changes during 1986–1996. *J. Mar. Syst.,* **19,** 113–135.

Simonot, J.-Y. R., and C. Gautier, 1989: Satellite estimates of surface evaporation in the Indian Ocean during the 1979 monsoon. *Ocean Air Interact.,* **1,** 239–256.

Smith, S. R., D. M. Legler, and K. V. Verzone, 2001: Quantifying uncertainties in NCEP reanalyses using high-quality research vessel observations. *J. Climate,* **14,** 4062–4072.

Sun, B., L. Yu, and R. A. Weller, 2003: Comparisons of surface meteorology and turbulent heat fluxes over the Atlantic: NWP model analyses versus moored buoy observations. *J. Climate,* **16,** 679–695.

Taylor, P. K., Ed., 2000: Intercomparison and validation of ocean-atmosphere energy flux fields. Joint WCRP/SCOR Working Group on Air Sea Fluxes Rep. WCRP-112, 305 pp.

Toole, J. M., H.-M. Zhang, and M. J. Caruso, 2004: Time-dependent internal energy budgets of the tropical warm water pools. *J. Climate,* in press.

Vesperini, M., 1998: Humidity in the ECMWF model: Monitoring of operational analyses and forecasts using SSM/I observations. *Quart. J. Roy. Meteor. Soc.,* **124,** 1313–1328.

Wang, W., and M. J. McPhaden, 2001: What is the mean seasonal cycle of surface heat flux in the equatorial Pacific? *J. Geophys. Res.,* **106,** 837–857.

Webster, P., and R. Lukas, 1992: TOGA COARE: The Coupled Ocean–Atmosphere Response Experiment. *Bull. Amer. Meteor. Soc.,* **73,** 1377–1416.

Weller, R. A., and S. P. Anderson, 1996: Surface meteorology and air–sea fluxes in the western equatorial Pacific warm pool during the TOGA COARE. *J. Climate,* **9,** 1959–1990.

——, M. F. Baumgartner, S. A. Josey, A. S. Fisher, and J. C. Kindle, 1998: Atmospheric forcing in the Arabian Sea during 1994–1995 observations and comparisons with climatology models. *Deep-Sea Res.,* **45,** 1961–1999.

Wentz, F. J., 1992: Measurement of oceanic wind vector using satellite microwave radiometers. *IEEE Trans. Geosci. Remote Sens.,* **30,** 960–972.

——, 1997: A well-calibrated ocean algorithm for SSM/I. *J. Geophys. Res.,* **102,** 8703–8718.

White, G. H., 1995: An intercomparison of precipitation and surface fluxes from operational NWP analysis/forecast systems. WMO CAS/JSC Working Group on Numerical Experimentation Rep. 22, WMO/TD-723, 33 pp.

Yu, L., and J. J. O'Brien, 1991: Variational estimation of the wind stress drag coefficient and the oceanic eddy viscosity profile. *J. Phys. Oceanogr.,* **21,** 709–719.

——, and ——, 1995: Variational data assimilation for determining the seasonal net surface heat flux using a tropical Pacific Ocean model. *J. Phys. Oceanogr.,* **25,** 2319–2343.

——, B. Sun, and R. A. Weller, 2002: Developing daily latent and sensible heat fluxes for the Atlantic Ocean by synthesizing satellite retrievals and outputs of numerical weather prediction models (1988–1999). WHOI Tech. Rep., 38 pp, and 14 figures.

Zeng, X., M. Zhao, and R. E. Dickinson, 1998: Intercomparison of bulk aerodynamic algorithms for the computation of sea surface fluxes using the TOGA COARE and TAO data. *J. Climate,* **11,** 2628–2644.